J|A|C|S
ARTICLES
Published on Web 00/00/0000

# Divalent Osmium Complexes: Synthesis, Characterization, Strong Red Phosphorescence, and Electrophosphorescence

Brenden Carlson,† Gregory D. Phelan,† Werner Kaminsky,† Larry Dalton,*,†
Xuezhong Jiang,‡ Sen Liu,‡ and Alex K.-Y. Jen‡

*Contribution from the Departments of Chemistry and Materials Science and Engineering, University of Washington, Seattle, Washington 98195*

Received December 3, 2001. Revised Manuscript Received June 3, 2002

***Abstract:*** We report new divalent osmium complexes that feature strong red metal-to-ligand-charge-transfer (MLCT) phosphorescence and electrophosphorescence. The general formula of the complexes is Os(II)-$(N-N)_2L-L$, where N−N is either a bipyridine or a phenanthroline and L−L is either a phosphine or an arsine. New polypyridyl ligands synthesized are 4,4′-di(biphenyl)-2,2′-bipyridine (**15**) and 4,4′-di(diphenyl ether)-2,2′-bipyridine (**16**), and the 1,10-phenanthroline derivatives synthesized are 4,7-bis(*p*-methoxyphenyl)-1,10-phenanthroline (**17**), 4,7-bis(*p*-bromophenyl)-1,10-phenanthroline (**18**), 4,7-bis(4′-phenoxybiphen-4-yl)-1,10-phenanthroline (**19**), and 4,7-bis(4-naphth-2-ylphenyl)-1,10-phenanthroline (**20**). 4,4′-Diphenyl-2,2′-bipyridine (**21**) and 4,7-diphenyl-1,10-phenanthroline (**22**) were also used in these studies. Strong $\pi$-acid ligands used were 1,2-bis(diphenylarseno)ethane (**23**), *cis*-1,2-bis(diphenylphosphino)ethylene (**24**), and *cis*-1,2-vinylenebis(diphenylarsine) (**25**). Ligand **25** is used for the first time in these types of luminescent osmium complexes. These compounds feature strong MLCT absorption bands in the visible region and strong red phosphorescent emission ranging from 611 to 651 nm, with quantum efficiency up to 45% in ethanol solution at room temperature. Red organic light-emitting diodes (OLEDs) were successfully fabricated by doping the Os(II) complexes into blend of poly(*N*-vinylcarbazole) (PVK) and 2-*tert*-butylphenyl-5-biphenyl-1,3,4-oxadiazole (PBD). Brightness over 1400 cd/m$^2$ for a double-layer device has been reached, with a turn-on voltage of 8 V. The maximum external quantum efficiency was 0.64%. Commission Internationale de l'Eclairage (CIE) chromaticity coordinates (*x*, *y*) of the red electrophosphorescence from the complexes are (0.65, 0.34), which indicates pure red emission.

## Introduction

Rapid growth in the use of organic light-emitting devices (OLED) is expected in the coming years[1] due to their potential application in large-screen flat-panel displays.[2−4] For full-color displays, efficient OLEDs emitting three primary colors, i.e., blue, green, and red, are required. Pure red color has been intrinsically difficult to obtain from conjugated polymers and small molecules. This is due to difficulty in tuning the energy levels of the compounds and the energy gap law, which describes the decrease in luminescence intensity with red-shifting emission. Because of the expected growth in the application of OLEDs, there has been much effort put into the development of novel emitters for use in OLED applications. Recently there has been interest in the use of triplet-emitting compounds primarily focusing on trivalent iridium complexes,[5,6] various platinum porphyrin derivatives,[7,8] and divalent ruthenium (Ru) complexes such as Ru(II)tris(2,2′-bipyridine) [Ru(II)-tris(**26**)].[9−11] Until recently,[12−15] osmium (Os) complexes have largely been ignored for applications in OLEDs. One reason for this is that Os tris(polypyridyl) complexes in general have low quantum yields when compared to their Ru(II) counterparts.

It has been reported that tris(polypyridyl)Os(II) complexes have very low quantum yields (on the order of 0.1%) and very short emission lifetimes (on the order of 50 ns).[16] The emission

* Corresponding author.
† Department of Chemistry.
‡ Department of Materials Science and Engineering.

(1) Allen, K. *Solid State Technol.* **2001**, *August*, 42.
(2) Burroughes, J. H.; Bradley, D. D. C.; Brown, A. R.; Marks, R. N.; Mackay, K.; Friend, R. H.; Burn, P. L.; Holmes, A. B. *Nature* **1990**, *347*, 539.
(3) Friend, R. H.; Gymer, R. W.; Holmes, A. B.; Burroughes, J. H.; Marks, R. N.; Taliani, C.; Bradley, D. D. C.; Dos Santos, D. A.; Bredas, J. L.; Logdlund, M.; Salaneck, W. R. *Nature* **1999**, *397*, 121.
(4) Bernius, M. T.; Inbasekaran, M.; O'Brien, J.; Wu, W. *Adv. Mater*. **2000**, *12* (23), 1737.
(5) Chen, F.; Yang, Y.; Thompson, M. E.; Kido, J. *Appl. Phys. Lett.* **2002**, *80* (13), 2308.
(6) Lamansky, S.; Djurovich, P.; Murphy, D.; Abdel-Razzaq, F.; Lee, H.; Adachi, C.; Burrows, P. E.; Forrest, S. R.; Thompson, M. E. *J. Am. Chem. Soc.* **2001**, *123* (18), 4304.
(7) Kwong, R. C.; Sibley, S.; Dubovoy, T.; Baldo, M.; Forrest, S. R.; Thompson, M. E. *Chem. Mater*. **1999**, *11* (12), 3709.
(8) Chang, S. E.; He, G.; Chen, F. C.; Guo, T. F.; Yang, Y. *Appl. Phys. Lett.* **2001**, *79*, 2088.
(9) Handy, E. S.; Pal, A. J.; Rubner, M. F. *J. Am. Chem. Soc.* **1999**, *121* (14), 3525.
(10) Liu, C.-Y.; Bard, A. J. *J. Am. Chem. Soc*. **2002**, *124* (16), 4190−4191.
(11) Rudmann, H.; Shimada, S.; Rubner, M. F. *J. Am. Chem. Soc*. **2002**, *124* (17), 4918.
(12) Carlson, B.; Jiang, X. Z.; Liu, M.; Liu, S.; Jen, A. K.-Y.; Dalton, L. *Polym. Mater. Sci. Eng.* **2002**, *86*, 210.
(13) Jiang, X. Z.; Jen, A. K.-Y.; Carlson, B.; Dalton, L. R. *Appl. Phys. Lett*. **2002**, *80* (5), 713.
(14) Bernhard, S.; Gao, X.; Malliaras, G. G.; Abruna, H. D. *Adv. Mater*. **2002**, *14* (6), 433.
(15) Ma, Y. G.; Zhang, H. Y.; Shen, J. C.; Che, C. M. *Synth. Met.* **1998**, *94*, 245.

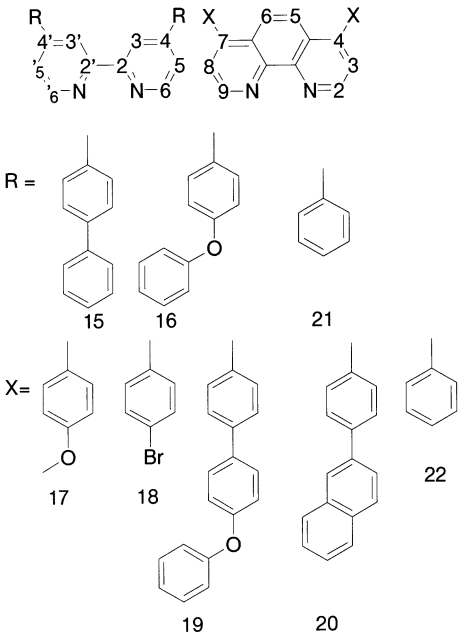


***Figure 1.*** Polypyridyl ligands and numbering position on the ring: 2,2′-bipyridine is on the left and 1,10-phenanthroline is on the right.

bands of tris(polypyridyl) Os(II) complexes are greatly red-shifted from their Ru(II) counterparts and occur in the near-infrared, which makes them unsuitable for use as OLEDs. This is due to the fact that Os(II) is more easily oxidized than Ru(II). According to the gap law, decreasing the energy difference between the excited and ground states enhances nonradiative decay of the excited state. Thus, red-shifting the emission band could decrease emission quantum yields; however, this does not have to be the case.

In designing a synthetic strategy, the above-discussed problems must be taken into account. It has been repeatedly shown that the use of phenyl groups on the polypyridyl ligand (Figure 1) greatly increases quantum yields. For example, the quantum yield for emission of Ru(II)tris(phenanthroline) is 1.9%, while the yield for Ru(II)tris(**22**) is 36.6%,[17] despite a red shift in emission from 595 nm for the phenanthroline complex to 610 nm for the **22** complex. Similar results can be observed for Ru(II) tris complexes of both **21** and **26**. The reason for this is that the phenyl groups undergo a conformational change[18] in the excited state, contributing to and extending to the $\pi$ system. In this conformation there is a barrier to C−C bond rotation due to the extended $\pi$ system. This reduces C−C bond rotation and vibration of the substituent, both of which may lead to an increase in nonradiative decay. This barrier would not exist for other substituents such as a methyl or other aliphatic groups. The substitution also replaces a C−H bond vibration para to the nitrogen, which may quench luminescence. Therefore, phenyl or other aromatic derivatives of polypyridyls were used in this study to increase quantum yields.

While Os(II)tris(**22**) and similar derivatives exhibit some increase in quantum yield, the emission is still in the infrared, making them unsuitable for use as OLEDs. Meyer and coworkers[19,20] showed that that the use of strong $\pi$ acid ligands

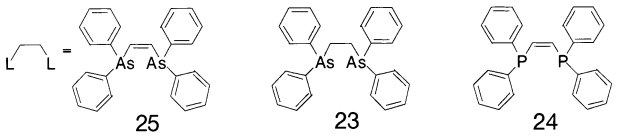


***Figure 2.*** Structures of strong $\pi$ acid ligands.

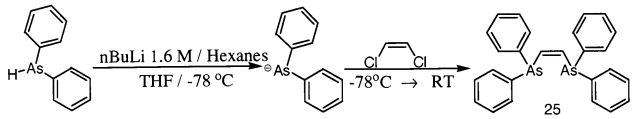


***Figure 3.*** Synthetic scheme for *cis*-1,2-vinylenebis(diphenylarsine).

(such as arsines, phosphines, DMSO, CN, and CO; see Figure 2) in combination with polypyridyl ligands may yield Os(II) complexes with quantum yields approaching 24%. These strong $\pi$ acid ligands (arsines and phosphines) strongly back-bond with the Os, but their $\sigma^*$ or d accepting orbitals are very high in energy[21] compared to the polypyridyl $\pi^*$; thus, the charge transfer to ligand bands are dominantly Os ($t_{2g}$) → bpy ($\pi^*$). By reducing the number of polypyridyl ligands, there is less ability to accept an electron; thus, there is a shift to higher energy in the absorption and emission bands from the tris(polypyridyl) counterparts. This makes the mixed-ligand system suitable for OLED applications by blue-shifting the emission from the infrared (750−850 nm) for the Os(II)tris(polypyridyl) complexes to orange-red (600−650 nm) for the mixed ligand system. These changes in structure cause an increase in radiative decay and leads to emission yields up to 45%.

Using triplet-based emitting centers in organic and polymer OLEDs eliminates the 25% limit for maximum internal quantum efficiency, which is the expected singlet exciton fraction generated by electrical injection, and potentially allows for displays with 100% internal quantum efficiency.[22] Strong back-bonding with a metal center, which exhibits a large spin−orbit coupling constant, facilitates intersystem crossing by breaking down the spin selection rules, thus leading to stronger triplet-state emission. Improved phosphorescence provides a possibility to design a high-efficiency OLED device. Triplet-harvesting red and green OLEDs based on Pt and Ir complexes have demonstrated very high external quantum efficiency.[23−27] Europium complexes also show triplet emission and have been used in red OLEDs.[28−30] The characteristic of the lowest excited states (triplet states) of these heavy-metal complexes can be systematically varied from largely ligand-centered (LC) to metal-to-

(16) Fetterolf, M. L.; Offen, H. W. *J. Phys. Chem.* **1985**, *89* (15), 3320.
(17) Alford, P.; Cook, M.; Lewis, A.; McAuliffe, G.; Skarda, V.; Thomson, A.; Glasper, J.; Robbins, D. *J. Chem. Soc., Perkin Trans. 2* **1985**, 705.
(18) Damrauer, N.; McCusker, J. K. *Inorg. Chem.* **1999**, *38*, 4268.
(19) Kober, E.; Caspar, J.; Sullivan, P.; Meyer, T. *Inorg. Chem.* **1988**, *27*, 4587.
(20) Kober, E. M.; Sullivan, B. P.; Dressick, W. J.; Caspar, J. V.; Meyer, T. J. *J. Am. Chem. Soc.* **1980**, *102* (24), 7383.
(21) *Periodic Correlations*; Rich, R. L., Ed.; Benjamin: New York, 1965; p 6.
(22) Adachi, C.; Baldo, M.; Thompson, M. E.; Forrest, S. R. *J. Appl. Phys.* **2001**, *90* (10), 5048.
(23) Baldo, M. A.; O'Brien, D. F.; You, Y.; Shoustikov, A.; Sibley, S.; Thompson, M. E.; Forrest, S. R. *Nature* **1998**, *395*, 151.
(24) Kwong, R. C.; Sibley, S.; Dubovoy, T.; Baldo, M. A.; Forrest, S. R.; Thompson, M. E. *Chem. Mater.* **1999**, *11*, 3709.
(25) Baldo, M. A.; Lamansky, S.; Burrows, P. E.; Thompson, M. E.; Forrest, S. R. *Appl. Phys. Lett.* **1999**, *75*, 4.
(26) Tsutsui, T.; Yang, M.; Yahiro, M.; Nakamura, K.; Watanabe, T.; Tsuji, T.; Fukuda, Y.; Wakimoto, T.; Miyaguchi, S. *Jpn. J. Appl. Phys.* **1999**, *38*, L1502.
(27) Adachi, C.; Baldo, M. A.; Forrest, S. R.; Lamansky, S.; Thompson, M. E.; Kwong, R. C. *Appl. Phys. Lett.* **2001**, *78*, 1622.
(28) Kido, J.; Hayase, H.; Hongawa, K.; Nagai, K.; Okuyama, K. *Appl. Phys. Lett.* **1994**, *65*, 2124.
(29) McGehee, M. D.; Bergstedt, T.; Zhang, C.; Saab, A. P.; O'Regan, M. B.; Bazan, G. C.; Srdanov, V. I.; Heeger, A. J. *Adv. Mater.* **1999**, *11*, 1349.
(30) Jiang, X.; Jen, A. K.-Y.; Huang, D.; Phelan, G.; Londergan, T.; Dalton, L. *Synth. Met.* **2002**, *125*, 331−336.

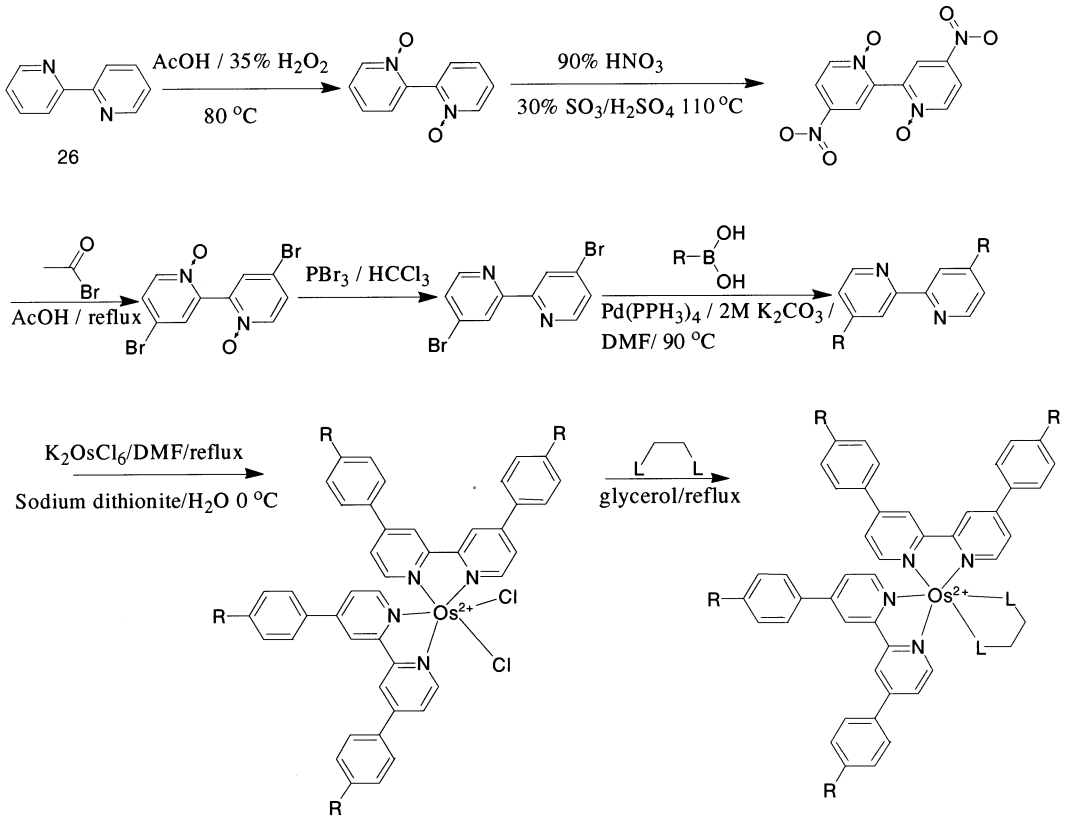


| Complex | R | L-L |
|---|---|---|
| 1 |  | 23 |
| 2 |  | 24 |
| 3 |  | 25 |
| 4 | 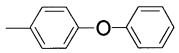 | 25 |
| 5 | 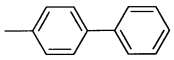 | 23 |
| 6 | 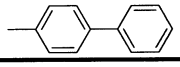 | 25 |

***Figure 4.*** Synthetic scheme for 4,4′-dibromo-2,2′-bipyridine and structures of Os(II) complexes based on resulting ligands.

ligand-charge-transfer (MLCT) character. The triplet emission character depends on the strength of the back-bonding between the metal center and the ligand and the relative energies of the $\pi^*$ (LC) transition vs the d$\pi^*$ (MLCT) transition. The emission of Eu complexes (sharp bands at around 615 nm) is completely inner-shell electronic f to d transitions and is determined by the energetics of the central $Eu^{3+}$ ion.[31] The emission from Pt(II) porphyrins is ligand-based, and Ir(III) complexes are largely ligand-based, though MLCT complexes have been reported for some Ir complexes as well.[25] Luminescence of the Os(II) complexes being reported is from the MLCT state. Furthermore, these third-row heavy-metal complexes tend to be thermally, chemically, and photochemically robust, which is favorable for device stability. Extremely long device lifetime has been reported for a triplet OLED device with platinum octaethylporphyrin (PtOEP) as LC emitting center with a 298 K triplet lifetime of ~50 $\mu$s. The long device lifetime is speculated to be an intrinsic property of electrophosphorescent OLEDs, where radiative phosphors significantly shorten the lifetime of potentially reactive triplet states in the conductive host material.[32] In Os complexes, due to strong back-bonding from Os to the ligands, the triplet MLCT emission has a very short lifetime (0.4−2 $\mu$s). Although Eu, Pt, and Ir complexes have been studied to some extent, the application of Os complexes in OLED has barely been explored.[12−15] In this paper we report the use of various novel Os(II) complexes featuring strong red emission and high quantum yields in OLED devices.

(31) Richardson, F. S. *Chem. Rev.* **1982**, *82*, 541.

(32) Burrows, P. E.; Forrest, S. R.; Zhou, T. X.; Michalski, L. *Appl. Phys. Lett.* **2000**, *76*, 2493.

## Experimental Section

**Syntheses of Materials.** 1,2-Bis(diphenylarseno)ethylene (**23**) and *cis*-1,2-bis(diphenylphosphino)ethane (**24**) were purchased from either Aldrich or Alfa and recrystallized 3 times from butanol before use. 4,4′-Diphenyl-2,2′-bipyridine (**21**) and bathophenanthroline (**22**) were purchased from GFS Chemicals. Compound **21** was ~50% pure and was purified by repeated washings and recrystallization from dimethylformamide (DMF) to yield 2.3 g out of 15 g purchased. Potassium hexachloroosmiate was purchased from Alfa.

**cis-1,2-Vinylenebis(diphenylarsine) (25)** (Figure 3) was prepared by a modification of a previous method, resulting in an improved yield of product.[33] Diphenylarsine (Organometallics, 25.00 g, 108.6 mmol) was used as received and was added to 400 mL of freshly dried (sodium/benzophenone) tetrahydrofuran (THF). The solution was stirred under nitrogen and cooled to −78 °C in an acetone/dry ice bath. To this solution was added *n*-butyllithium (1.6 M in hexane, 1.05 equiv, 114.1 mmol). The solution was allowed to stir for 1 h. The acetone bath was then removed and *cis*-dichloroethylene (TCI-America, 10.66 g, 110.0 mmol) was added. The solution was allowed to slowly warm to 18.5 °C and react overnight. Water was added and the THF was removed by rotary evaporation under vacuum at 40 °C. The water was removed by filtration and the solid material was washed with large amounts of deionized water. The sample was dried under vacuum and then recrystallized three times from butanol. Yield: 23.97 g (91%). $^1$H NMR (DMSO): 7.63 (s, 2H), 7.35 (20H). Anal. Calcd: C, 64.48%; H, 4.58%. Found: C, 64.10%; H, 4.28%.

**4,4′-Dibromo-2,2′-bipyridine** (Figure 4) was prepared by an adaptation and combination of the methods reported by Haginiwa[34] and Maerker and Chase.[35]

**4,4′-Di(biphenyl)-2,2′-bipyridine (15)** was synthesized from a palladium-catalyzed Suzuki cross-coupling reaction of 4,4′-dibromo-2,2′-bipyridine and biphenyl-4-boronic acid neopentyl glycol ester. $^1$H NMR ($DCCl_3$) as a Ru(II)(heptafluorobutyrate)$_2$ [Ru(II)(HFB)$_2$] complex: 9.08 (d, 6H), 7.97 (m, 18H), 7.80 (m, 18H), 7.61 (m, 12H), 7.45 (m, 18 H).

**4,4′-Bis(diphenyl ether)-2,2′-bipyridine (16)** was made following the same procedure as **15**: Yield 0.95 g (30.4%). $^1$H NMR (DMSO): 8.750 (d, 2H), 8.631 (m, 4H), 7.904 (m, 4H), 7.800 (m, 4H), 7.459 (t, 2H), 7.147 (m, 8H).

**4,7-Bis(*p*-methoxyphenyl)-1,10-phenanthroline (17) and 4,7-bis-(*p*-bromophenyl)-1,10-phenanthroline (18).** Syntheses of these compounds have been reported previously.[17]

Phenanthroline derivatives **19** and **20** were synthesized from **18.**

**4,7-Bis(4′-phenoxybiphenyl-4-yl)-1,10-phenanthroline (19)** was made following the same procedure as **15** and was recrystallized from benzene to give a colorless crystalline solid. $^1$H NMR (DMSO): 9.20 (d, 2H), 8.88−7.65 (m, 18H), 7.45 (t, 4H), 7.25−7.06 (m, 8H).

**4,7-Bis(4-naphth-2-ylphenyl)-1,10-phenanthroline (20)** was made following the same procedure as **15** and was recrystallized from DMF to give a colorless crystalline solid. $^1$H NMR ($DCCl_3$): 9.29 (d, 2H), 8.14 (s, 2H), 8.03−7.75 (m, 14 H), 7.72−7.63 (m, 6H), 7.57−7.46 (m, 4H).

**General Procedure[19] for Synthesis of Osmium Complexes.** The osmium complexes were synthesized by reacting 1.000 g (2.08 mmol) of $K_2OsCl_6$ with 2.05 equiv of polypyridyl (N−N) ligand in 25 mL of refluxing DMF (Aldrich) under an inert atmosphere for 3 h. The resulting solution was filtered, washed with DMF, cooled to 0 °C, and then added dropwise to a water solution of sodium dithionite (2.00 g in 400 mL) at 0 °C. The resulting purple precipitate of Os(N−N)$_2$Cl$_2$ was filtered and washed with deionized water. Os(N−N)$_2$Cl$_2$ was reacted with 1.05 equiv of arsine or phosphine ligand (**23**, **24**, or **25**) in a refluxing mixture of 2,2′-ethoxyethoxyethanol (Aldrich) and glycerol (75:25 by volume) for 2 h under an inert atmosphere. The complexes were precipitated by dropwise addition to a water solution of the appropriate counterion: tosylate (Ts), triflate (Tf), heptafluorobutyrate (HFB), and $PF_6$. The complex structures are shown in Figures 4 and 5. Elemental analysis data, mass spectrometry results, and yields

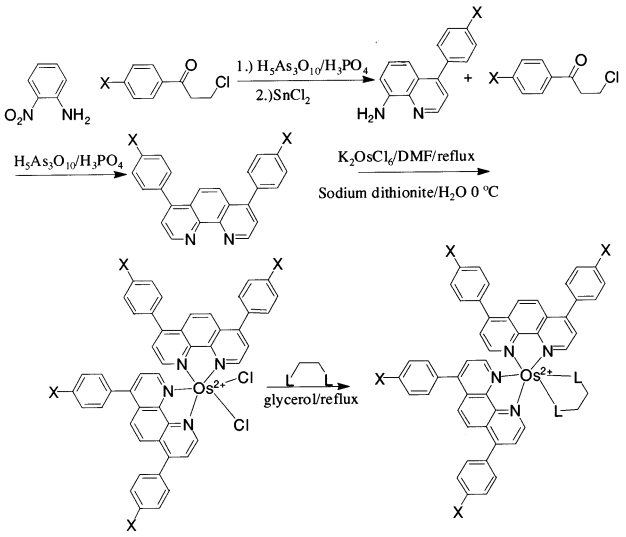


| Complex | X | L-L |
|---|---|---|
| **7** | H | 24 |
| **8** | H | 25 |
| **9** | O-Me | 23 |
| **10** | O-Me | 24 |
| **11** | O-Me | 25 |
| **12** | Br | 25 |
| **13** | 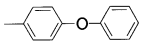 | 25 |
| **14** | 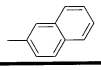 | 25 |

***Figure 5.*** Synthetic scheme for aromatic 4,7-substituted 1,10-phenanthrolines and structures of Os(II) complexes based on resulting ligands.

***Table 1.*** Elemental Analysis Data

| | calculated | | | found | | | | |
|---|---|---|---|---|---|---|---|---|
| compd | C | H | N | C | H | N | mass | yield (%) |
| **1** | 54.49 | 3.28 | 3.26 | 54.65 | 3.36 | 3.30 | 647.1[a] | 90 |
| **2** | 57.49 | 3.34 | 3.44 | 58.00 | 3.41 | 3.33 | 602.7[a] | 85 |
| **3** | 54.41 | 3.42 | 3.52 | 54.51 | 3.48 | 3.36 | 646.1[a] | 94 |
| **4** | 58.89 | 3.60 | 2.86 | 59.01 | 3.59 | 2.88 | 830.2[a] | 90 |
| **5** | 60.54 | 3.59 | 2.77 | 59.92 | 3.34 | 2.70 | 646.1[a] | 90 |
| **6** | 60.88 | 3.73 | 2.96 | 61.01 | 4.02 | 2.85 | 798.2[a] | 89 |
| **7** | 58.91 | 3.51 | 3.62 | 58.78 | 3.52 | 3.66 | 626.2[a] | 92 |
| **8** | 55.75 | 3.32 | 3.42 | 56.05 | 3.34 | 3.44 | 670.1[a] | 90 |
| **9** | 61.26 | 4.36 | 3.11 | 61.36 | 4.41 | 3.05 | 731.2[a] | 89 |
| **10** | 64.47 | 4.47 | 3.27 | 64.57 | 4.65 | 3.25 | 686.2[a] | 95 |
| **11** | 61.33 | 4.25 | 3.11 | 61.64 | 4.33 | 3.12 | 730.1[a] | 92 |
| **12** | 51.56 | 3.31 | 2.87 | 52.01 | 3.38 | 2.88 | 827.9[a] | 89 |
| **13** | 69.38 | 4.28 | 2.38 | 69.07 | 4.36 | 2.44 | 1006.1[a] | 93 |
| **14** | 70.25 | 4.33 | 2.56 | 70.56 | 4.32 | 2.48 | 922.7[a] | 88 |
| **15** | 88.67 | 5.25 | 6.08 | 89.06 | 5.32 | 6.21 | 461.6[b] | 51 |
| **16** | 82.91 | 4.91 | 5.69 | 83.09 | 4.99 | 5.77 | 493.2[b] | 30 |
| **17** | 79.57 | 5.14 | 7.14 | 79.45 | 5.26 | 7.20 | 393.3[b] | 32 |
| **18** | 58.81 | 2.88 | 5.71 | 58.88 | 2.79 | 5.75 | 490.9[b] | 50 |
| **19** | 86.20 | 4.82 | 4.19 | 86.32 | 4.98 | 4.28 | 669.3[b] | 64 |
| **20** | 90.38 | 4.83 | 4.79 | 90.45 | 4.86 | 4.81 | 561.5[b] | 68 |
| **25** | 64.48 | 4.58 | 0.00 | 64.10 | 4.28 | 0.08 | c | 91 |

[a] *m*/2*z*. [b] *m*/*z*. [c] Highly fragmented, no *m*/*z*.

(33) Mitchener, J. P.; Aguiar, A. M. *Org. Prep. Proced.* **1969**, *1* (4), 259−261.
(34) Haginiwa, J. *Yakugaku Zasshi* **1955**, *6*, 731.
(35) Maerker, G.; Chase, F. *J. Am. Chem. Soc.* **1958**, *80*, 5.

| | |
|---|---|
| **1** | [Os(II)bis(4,4′-diphenyl-2,2′-bipyridine) 1,2-bis(diphenylarseno)ethane]$^{2+}$ |
| **2** | [Os(II)(4,4′-diphenyl-2,2′-bipyridine)$_2$ *cis*-1,2-bis(diphenylphosphino)ethylene]$^{2+}$(HFB)$_2$ |
| **3** | [Os(II)(4,4′-diphenyl-2,2′-bipyridine)$_2$ *cis*-1,2-vinylenebis(diphenylarsine)]$^{2+}$(Tf)$_2$ |
| **4** | [Os(II)(4,4′-bis(*p*-diphenyl ether)-2,2′-bipyridine)$_2$ *cis*-1,2-vinylenebis(diphenylarsine)]$^{2+}$(Tf)$_2$ |
| **5** | [Os(II)(4,4′-bis(*p*-biphenyl)-2,2′-bipyridine)$_2$ 1,2-bis(diphenylarseno)ethane]$^{2+}$(HFB)$_2$ |
| **6** | [Os(II)(4,4′-bis(*p*-biphenyl)-2,2′-bipyridine)$_2$ *cis*-1,2-vinylenebis(diphenylarsine)]$^{2+}$(Tf)$_2$ |
| **7** | [Os(II)(bathophenanthroline)$_2$ *cis*-1,2-bis(diphenylphosphino)ethylene]$^{2+}$(Tf)$_2$ |
| **8** | [Os(II)(bathophenanthroline)$_2$ *cis*-1,2-vinylenebis(diphenylarsine)]$^{2+}$(Ts)$_2$ |
| **9** | [Os(II)(4,7-bis(*p*-methoxyphenyl)-1,10-phenanthroline)$_2$1,2-bis(diphenylarseno)ethane]$^{2+}$(Ts)$_2$ |
| **10** | [Os(II)(4,7-bis(*p*-methoxyphenyl)-1,10-phenanthroline)$_2$ *cis*-1,2-bis(diphenylphosphino)ethylene]$^{2+}$(Ts)$_2$ |
| **11** | [Os(II)(4,7-bis(*p*-methoxyphenyl)-1,10-phenanthroline)$_2$ *cis*-1,2-vinylenebis(diphenylarsine)]$^{2+}$(Ts)$_2$ |
| **12** | [Os(II) (4,7-bis(*p*-bromophenyl)-1,10-phenanthroline)$_2$ *cis*-1,2-vinylenebis(diphenylarsine)]$^{2+}$(Ts)$_2$ |
| **13** | [Os(II)(4,7-bis(4′-phenoxybiphenyl-4-yl)-1,10-phenanthroline)$_2$ *cis*-1,2-vinylenebis(diphenylarsine)]$^{2+}$(Ts)$_2$ |
| **14** | [Os(II)(4,7-bis(4-naphth-2-ylphenyl)-1,10-phenanthroline)$_2$ *cis*-1,2-vinylenebis(diphenylarsine)]$^{2+}$(Ts)$_2$ |

are presented in Table 1. More detailed synthesis and characterization data can be found in the Supporting Information.

**Characterization.** Elemental analyses were carried out by Oneida Research Services, Inc, Whitesboro, NY. UV−vis absorption spectra were measured on a Shimadzu UV-1601 spectrophotometer. Quantitative measurements were obtained by using 1.000 cm path length quartz cells with absolute ethanol as the solvent. Electrospray mass spectroscopy was measured on either an Esquire-LC ion trap mass spectrometer (Bruker and Hewlett-Packard) or an Applied Biosystems Mariner ESI-TOF mass spectrometer. $^1$H NMR was carried out on a 200 MHz Bruker FT-NMR spectrometer.

Emission spectra of ethanol solutions were collected on a Perkin-Elmer LS50B fluorescence spectrophotometer. The wavelength sensitivity of the instrument was calibrated prior to measurements using a standard 20 W tungsten lamp of known output. All emission spectra were corrected to the calibration curve calculated from the known lamp output. The solutions were degassed using argon for 30 min before the measurement. Photoluminescence (PL) quantum yields to ±10% of the Os complexes ($\Phi_{Os}$) in ethanol solutions were obtained with Ru(II) tris-**22** dichloride as the standard, which has a known quantum yield of 0.366, from the following equation:[36]

$$\Phi_{Os} = \frac{\text{abs Ru}}{\text{area Ru}} \frac{\text{area Os}}{\text{abs Os}} \times 36.6\% \qquad (1)$$

where abs is the absorbance of the sample and area is the integration of the emission curve. Samples were excited through the LC state at 280 nm with absorption of 0.050. Temperature for the measurements was 25 ± 2 °C.

For lifetime measurement, the Os complexes were dissolved into a paint solution of FIB7[37,38] polymer (Figure 6) and trifluorotoluene. FIB7 is a very photostable polymer and does not absorb light above 235 nm. The solution was spray-painted onto a polished aluminum plate and dried at 50 °C. The samples were put into a sample holder,[38] placed under vacuum, and excited at 338 nm with a nitrogen pulse laser. The luminescence decay was monitored and the lifetime was calculated.[39] Samples for photodegradation and temperature dependence were prepared following the same procedures as for the lifetime measurements detailed above. A tungsten−halogen lamp filtered by a FIV-026 band-pass filter was used as the excitation source (400 nm, FWHM = 20 nm). The Power density was 925 $\mu$W cm$^{-2}$. The emission intensity was monitored with a photomultiplier tube.[37,38] The illumination for degradation was continuous and the temperature was set to 25 °C, while for temperature dependence the shutter time was 1 s and the temperature ranged from 5 to 50 °C.

**Device Fabrication and Testing.** OLED devices were fabricated on ITO substrates that were cleaned and treated with $O_2$ plasma before use. A layer of ∼40 nm thick hole-transport material (HTL), a tetraphenyldiamine-containing perfluorocyclobutane polymer (BTPD-PFCB) (Figure 6), was first fabricated by spin-coating the monomer from its 1,2-dichloroethane (DCE) solution and annealing at 225 °C under nitrogen atmosphere.[40] Then a layer of 3.0 wt % Os complex doped blend of poly(*N*-vinylcarbazole) and 2-(*t*-butyl)phenyl-5-biphenyl-1,3,4-oxadiazole (PVK:PBD, 70:30 by weight) or poly(2-vinylnaphthalene) and PBD (PVN:PBD, 70:30 by weight) was spin-coated from the corresponding DCE solution (∼12 mg/mL) at 2000 rpm. A layer of 30-nm-thick Ca was vacuum-deposited at below 1 × 10$^{-6}$ Torr through a mask in an argon-protected evaporator, and another layer of 120-nm-thick Ag was deposited as a protective layer. All testing was carried out in air at room temperature. Current−voltage characteristics were measured on a Hewlett-Packard 4155B semiconductor parameter analyzer. EL spectra were measured with an Oriel InstaSpec IV CCD camera or a Photo Research PR650 colorimeter. The EL emission power was measured by use of a Newport 2835-C multifunction optical meter in combination with a calibrated photodiode. Brightness was calculated from the emission power and EL spectra of the devices, assuming Lambertian distribution of the EL emission.[41] Thickness of the films was measured on a Sloan Dektak 3030 profilometer.

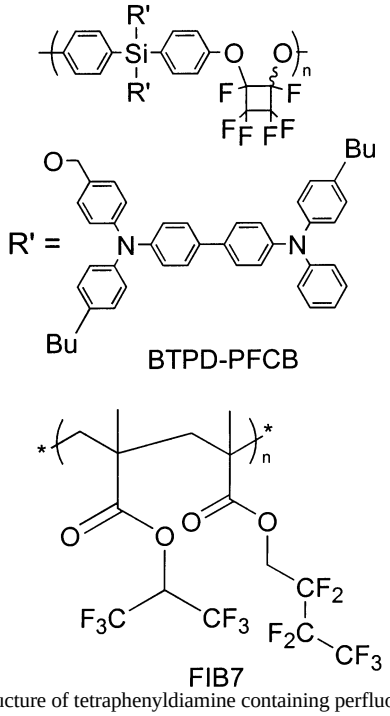


***Figure 6.*** Structure of tetraphenyldiamine containing perfluorocyclobutane polymer (BTPD-PFCB) and FIB7 polymer.

(36) Wallace, L.; Rillema, D. P. *Inorg. Chem.* **1993**, *32*, 3836.
(37) Puklin, E.; Carlson, B.; Gouin, S.; Costin, C.; Green, E.; Ponomarev, S.; Tanji, H.; Gouterman, M. *J. Appl. Polym. Sci.* **2000**, *77* (13), 2795.
(38) Carlson, B.; Gouterman, M. U.S. Patent 5,965,642, 1999.
(39) Coyle, L. Dissertation, University of Washington, 1999.
(40) Jiang, X. Z.; Liu, S.; Liu, M. S.; Ma, H.; Jen, A. K.-Y. *Appl. Phys. Lett.* **2000**, *76*, 2985.
(41) Greenham, N. C.; Friend, R. H.; Bradley, D. D. C. *Adv. Mater.* **1994**, *6*, 491.

**Table 2.** Crystallographic Data for the Structures Provided

| property | *cis*-1,2-vinylenebis-(diphenylarsine) | complex **3** | complex **12** |
|---|---|---|---|
| empirical formula | $C_{26}H_{22}As_2$ | $C_{84}H_{70}As_2N_4O_7OsS_2$ | $C_{90}H_{66}As_2Br_4Cl_6N_4O_6OsS_2$ |
| formula weight | 484.28 | 1651.60 | 2235.92 |
| temperature, K | 130(2) | 130(2) | 130(2) |
| wavelength, Å | 0.710 73 | 0.710 73 | 0.710 73 |
| crystal/color | prism/clear | plate/dark red | prism/dark red |
| crystal system | monoclinic | monoclinic | orthorhombic |
| space group | *Pc* **(no. 7)** | $P2_1/c$ (no. 14) | $P2_12_12$ (no. 18) |
| unit cell dimensions | | | |
| *a*, Å | 12.5920(4) | 18.329(5) | 14.5150(2) |
| *b*, Å | 5.6160(2) | 17.240(10) | 26.0710(3) |
| *c*, Å | 17.0320(6) | 22.048(9) | 11.1480(7) |
| α, deg | 90 | 90 | 90 |
| *β*, deg | 117.1651(13) | 99.055(11) | 90 |
| *γ*, deg | 90 | 90 | 90 |
| volume, Å$^3$ | 1071.59(6) | 6880(5) | 4218.6(3) |
| density, Mg/m$^3$ | 1.501 | 1.594 | 1.760 |
| reflections collected/unique | 14 847/4081 | 14 1517/7042 | 35 455/8380 |
| final *R* indices [$I > 2\sigma(I)$] | | | |
| *R*1 | 0.0376 | 0.0667 | 0.0554 |
| *wR*2 | 0.0851 | 0.0661 | 0.1171 |
| *R* indices (all data) | | | |
| *R*1 | 0.0431 | 0.1780 | 0.0853 |
| *wR*2 | 0.0872 | 0.0840 | 0.1276 |

**Table 3.** Bond Lengths for Free Ligand and Complexes **3** and **12**[a]

| complex | N1 | N2 | N3 | N4 | As1 | As2 |
|---|---|---|---|---|---|---|
| **3** | 2.054(9) | 2.094(8) | 2.011(11) | 2.057(9) | 2.3997(15) | 2.420(15) |
| **12** | 2.096(7) | 2.091(7) | 2.096(7) | 2.091(7) | 2.4165(9) | 2.4165(9) |

| arsenic | C(br) | C(Ph) | C(Ph) | C=C(br) |
|---|---|---|---|---|
| As1 | 1.956(5) | 1.971(4) | 1.973(5) | 1.308(7) |
| As1a | 1.8285 | 2.171(5) | 2.330(6) | 1.4581 |
| As2 | 1.955(5) | 1.972(5) | 1.976(4) | 1.308(7) |
| As2a | 1.8159 | 2.149(5) | 2.145(5) | 1.4581 |
| **3** | 1.932(11) | 1.930(10) | 1.945(11) | 1.296(11) |
| **12** | 1.895(10) | 1.946(9) | 1.790(3) | 1.374(19) |

[a] Bond lengths are given in angstroms; br = bridge; Ph = phenyl.

**Table 4.** C−As−C Bond Angles for Complexes for Free Ligand and Complexes **3** and **12**[a]

| arsenic | C(Ph)–As–C(br) | C(Ph)–As–C(br) | C(Ph)–As–C(Ph) |
|---|---|---|---|
| As1 | 98.9(2) | 96.1(2) | 96.88(2) |
| As1a | 88.35(14) | 82.15(15) | 81.87(2) |
| As2 | 96.9(2) | 97.6(2) | 95.81(2) |
| As2a | 86.21(2) | 81.23(15) | 89.82(2) |
| **3** | 103.7(5) | 103.6(5) | 101.3(4) |
| **12** | 105.9(5) | 101.0(5) | 101.8(6) |

| complex | C(Ph)–As–Os | C(Ph)–As–Os | C(br)–As–Os |
|---|---|---|---|
| **3** | 122.7(3) | 115.7(3) | 107.8(3) |
| **12** | 120.3(4) | 116.3(3) | 109.3(3) |

[a] Bond angles are given in degrees; br = bridge, Ph = phenyl.

**X-ray Diffraction.** Crystals of *cis*-1,2-vinylenebis(diphenylarsine) (**25**) were grown by dissolving the compound in hot 1-butanol and slowly cooling to room temperature. Crystals of complexes **3** and **12** were grown by dissolving the complex as the Ts salt in chloroform and then adding an equal volume of ethyl acetate. The solutions were then allowed to slowly evaporate. The crystals were mounted in random orientation on a glass fiber on a Kappa CCD diffractometer, Mo Kα ($\lambda$ = 0.710 73 Å). Measurements were performed at 130 ± 2 K. Cell constants and an orientation matrix for data collections were obtained by least-squares refinements of the diffraction data from up to 141 517 full and partial reflections. The structures were solved by direct methods with SIR97 and DIRDIFF, provided by the refinement package MaXus.[42] Missing atoms were found by difference Fourier synthesis. The non-hydrogen atoms were refined with anisotropic temperature factors. Scattering factors are from Waasmaier and Kirfel.[43] The structures were refined with SHELXL-97, and Ortep plots were generated with ORTEP32.[44] Tables 2−4 summarize the crystal data, collection information, and refinement data for these structures.

## Results and Discussion

**X-ray Diffraction.** Crystal structures (Figures 7−9) for **25** and complexes **3** and **12** are given. Compound **25** exhibits disorder of 88.9(2)% for As1C1C2As2 and 11.1(2)% for As1aC1aC2aAs2a. In addition, this noncentrosymmetric structure is complete by racemerized Flack-enantiopole parameter equal to 0.503(14). The bond angles around the arsenic vary greatly between the two conformations. As main-group elements beyond the second row of the periodic table are reluctant to hybridize, it is expected that the bonds that arsenic forms would

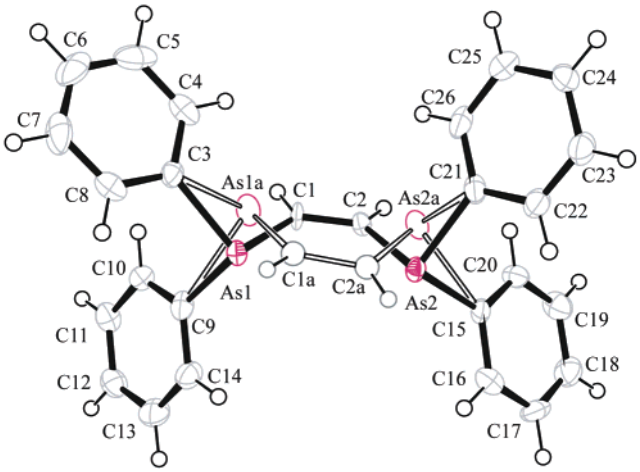


**Figure 7.** Crystal structure with 50% probability spheres for *cis*-1,2-vinylenebis(diphenylarsine).

(42) Mackay, S.; Edwards, C.; Henderson, A.; Gilmore, C.; Stewart, N.; Shankland, K.; Donald, A. *MaXus*, University of Glasgow, Scotland, 1997.
(43) Waasmaier, D.; Kirfel, A. *Acta Crystallogr. A* **1995**, *51*, 416.
(44) Farrugia, L. J. *Appl. Cryst.* **1997**, *30*, 565.

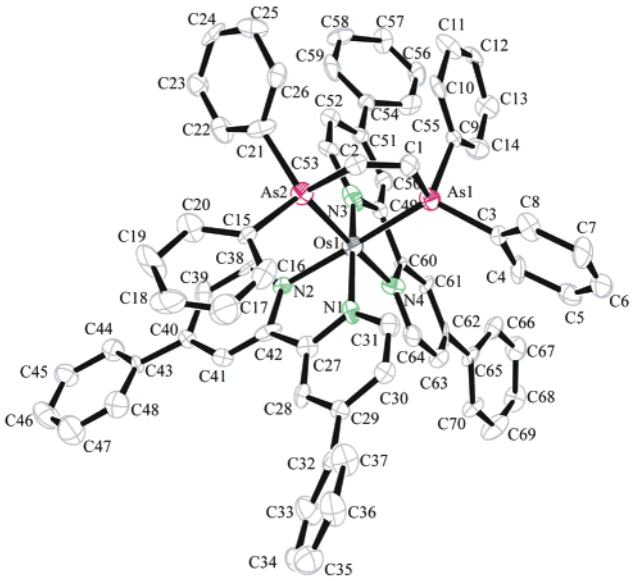


***Figure 8.*** Crystal structure with 50% probability spheres for complex **3**. Counterions and hydrogen have been removed for clarity.

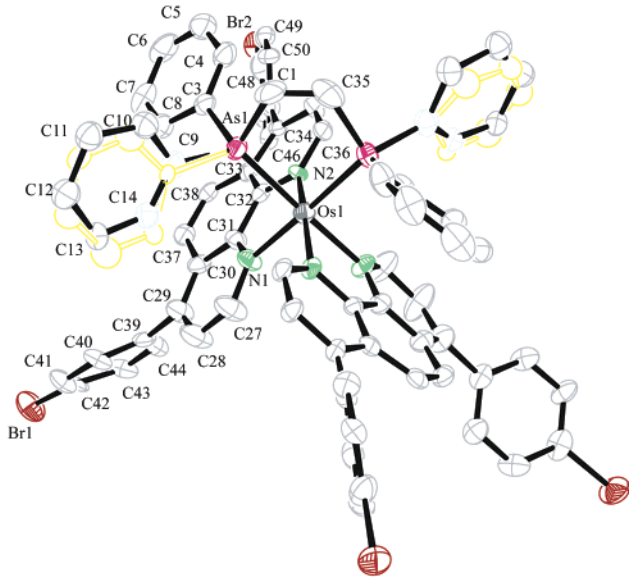


***Figure 9.*** Crystal structure with 50% probability spheres for complex **12**. Counterions and hydrogen have been removed for clarity.

be made with unhybridized p orbitals. The resulting bond angles would be 90° around arsenic. The conformer with probability 88.9(2)% had arsenic bond angles that ranged from 95.81(2)° to 98.9(2)°, or greater than expected with an average at 97.02(6)°. The conformer comprising 11.1(2)% of the structure of ligand **25** had bond angles of 81.23(15)−89.82(2)° with an average at 84.94(6)°, or smaller than expected. The average bond angle was 90.98(6)°, close to the 90° theoretically expected for organoarsenic compounds.

The structure for complexes **3** and **12** compares to a distorted octahedron. The bite angles for the ligands (**21**) in complex **3** were observed at 75.0(4)° and 77.0(4)° while the bite angle for the arsine ligand (**25**) was observed at 83.08(5)°. For complex **12**, the bite angles for both **18** were observed at 77.7(3)° while the arsine ligand was 83.28(5)°. The trans bond angles for complex **3** were as follows: N2−Os−As1, 172.0(3)°; N4−Os−As2, 177.7(3)°; and N1−Os−N3, 166.8(4)°. The trans bond angles for **12** were as follows: N(2)#1−Os(1)−N(2), 169.8(3)°; N(1)−Os(1)−As(1)#1, 178.1(2)°; N(1)#1−Os(1)−As(1), 178.1(2)°. A perfect octahedron would require the bite angles to be 90° and the trans bond angles to be 180°. Complex **12** is somewhat closer to ideal than **3** in that more of its trans bonds are closer to 180°. There was very little trans effect of the arsenic on the N−Os bond as the Os−N bond length is largely unaffected by the Os−N bond being trans to N or to As. This shows that the electron density being donated to osmium by the arsenic is in balance with removal through back-bonding. The bond angles around the arsenic deviate when complexed to the osmium from that of the uncoordinated ligand. The carbon−arsenic−carbon bond angles in both complexes **3** and **12** are broader than that of the free ligand and range from 101.0(5)° to 105.9(5)°. The osmium−arsenic−carbon bond angles range from 107.8(3)° to 122.7(3)°. The structure seems to be migrating to a distorted tetrahedron around the arsenic. A question arises if the arsenic is hybridizing when complexed to osmium or if steric forces are "pushing" the phenyl groups into a new geometry around the arsenic. Hybridization would be due to localization of the arsenic 4s "lone pair" in forming a bond with osmium. Examination of reported arsenic compounds gives the following bond angles: $AsH_3$, 91.8°; $AsF_3$, 95.97°; $AsCl_3$, 97.7°; $AsBr_3$, 97.7°; $AsI_3$, 99.7°; and $As(Ph)_3$, 100.1°.[45] Previous reports on the arsenic bond angles in this series and other similar arsenic compounds have concluded that hybridization of the arsenic is indeed taking place.[46−48] The arsenic bond angles in complexes **3** and **12** are larger than the series listed above and larger than that of the free ligand. However, the smallest of the arsenic bond angles in complexes **3** and **12**, 101.0(5)°, is close to what is observed for $As(Ph)_3$. The bond angle around the ethylene bridge (examined for signs of strain) on the ligand range were observed at 124.3(4)° and 123.2(4)° for structure 1 of the crystal and 120.1° and 123.7° for the second structure in the crystal lattice. These bond angles also remain nearly unchanged in the complexes **3** and **12** and were 122.7(3)° and 122.6(4)° for complex **3** and 118.9(3)° for complex **12**. It would seem that very little strain was placed upon the ethylene bridge by coordinating to osmium. If the arsine ligand is under strain, it is being observed only in the phenyl groups. However, there is space between the phenyl groups on the arsenic and the polypyridyl structures. It would be this type of interaction that would lead to steric effects that would change the geometry around arsenic. Evidence for this is librative disorder of the phenyl groups on the two arsenic atoms in structure **12**. From discussions in previous reports and the crystallographic evidence provided, it is proposed that p-character and possibly d character of the 4s on the arsenic is increasing due to the localization of electron pair contained therein in forming a bond with osmium. A structure study of a model compound that minimizes steric strain such as $(Cl)_4$-Os(IV)[**25**] could be used to determine if the arsenic is hybridizing.

**UV−Visible and Photoluminescence Spectroscopy.** Table 5 and Figures 10−13 summarize absorption and emission

(45) Norman, N. C. *Chemistry of Arsenic, Antimony, and Bismuth*; Blackie Academic: London, 1998.
(46) Svergun, V. I.; Babushkina, T. A.; Shvedova, G. N.; Kudryavtseva, L. V.; Semin, G. K. *Izv. Akad. Nauk SSSR, Ser. Khim.* **1970**, *2*, 482.
(47) Grechishishkin, V. S.; Yusupov, M. Z. *Zh. Strukt. Khim.* **1973**, *14* (6), 1028.
(48) Siddiqui, R. A.; Raj, P.; Saxena, A. K.; Dixit, S. K. *Synth. React. Inorg. Met.-Org. Chem.* **1996**, *26* (7), 1189.

***Table 5.*** Absorption Maxima for the Various Ligand and Charge Transfer Bands, Extinction Coefficients ($\epsilon$), and Emission Properties of the Os(II) Complexes Being Reported

| complex | LC (nm) ($\epsilon$) | $^1$MLCT (nm) ($\epsilon$) | $^3$MLCT (nm) ($\epsilon$) | emission[a] | $\tau$,[b] ns | $\Phi$[c] |
|---|---|---|---|---|---|---|
| **1** | 262 (52 000), 306 (60 000) | 405 (16 000) | 520 (3700) | 650 | 410 | 0.19 |
| **2** | 301 (68 000) | 382 (17 000) | 484 (4500) | 623 | 520 | 0.23 |
| **3** | 304 (70 000) | 397 (18 000) | 512 (4700) | 640 | 460 | 0.25 |
| **4** | 301 (62 000), 330 (63 000) | 402 (22 000) | 518 (4300) | 645 | 470 | 0.27 |
| **5** | 308 (89 000), 331 (87 000) | 408 (26 000) | 508 (10 000) | 651 | 430 | 0.22 |
| **6** | 304 (91 000), 334 (88 000) | 402 (28 000) | 522 (11 000) | 643 | 450 | 0.28 |
| **7** | 282 (66 000) | 378 (21 000) | 507 (sh, 4100) | 613 | 1810 | 0.33 |
| **8** | 279 (69 000) | 391 (22 000) | 524 (sh, 4000) | 623 | 1530 | 0.38 |
| **9** | 274 (66 000), 331 (45 000) | 397 (36 000) | 505 (sh, 9000) | 635 | 1200 | 0.27 |
| **10** | 269 (69 000), 327 (52 000) | 364 (50 000) | 487 (sh, 9000) | 611 | 1970 | 0.36 |
| **11** | 273 (71 000), 329 (43 000) | 391 (39 000) | 500 (sh, 8000) | 629 | 1550 | 0.45 |
| **12** | 290 (75 000) | 391 (28 000) | 500 (sh, 6300) | 635 | 1400 | 0.39 |
| **13** | 273 (101 000), 344 (49 000) | 393 (44 000) | 500 (sh, 7500) | 637 | 1310 | 0.40 |
| **14** | 283 (108 000), 331 (51 000) | 374 (52 000) | 500 (sh, 8400) | 637 | 1260 | 0.41 |

[a] Emission peak. [b] Luminescence lifetime. [c] Luminescence quantum yield.

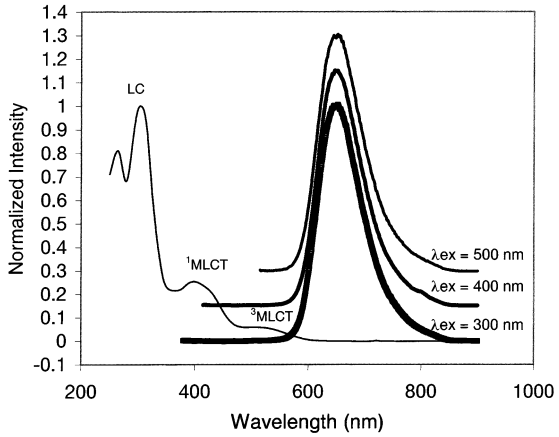


***Figure 10.*** Absorption of complex **3** and emission (640 nm) at three different excitations, 300, 400, and 500 nm. The emission curves are offset for clarity.

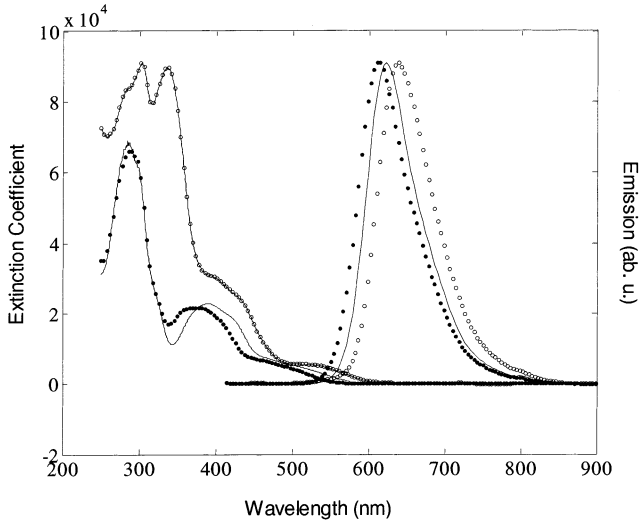


***Figure 11.*** Absorption ($\epsilon$) and emission of complexes **6** (○), **7** (●), and **8** (—).

properties of the complexes. Absorbance and emission spectra for complexes **1**, **2**, and **3** are reported in our previous report.[13] Complexes with bipyridyl ligands exhibit an adsorption band at >300 nm, while complexes with phenanthroline ligands exhibit an adsorption band at <290 nm. These bands are attributed to the $\pi-\pi^*$ transition centered on the ligand. These

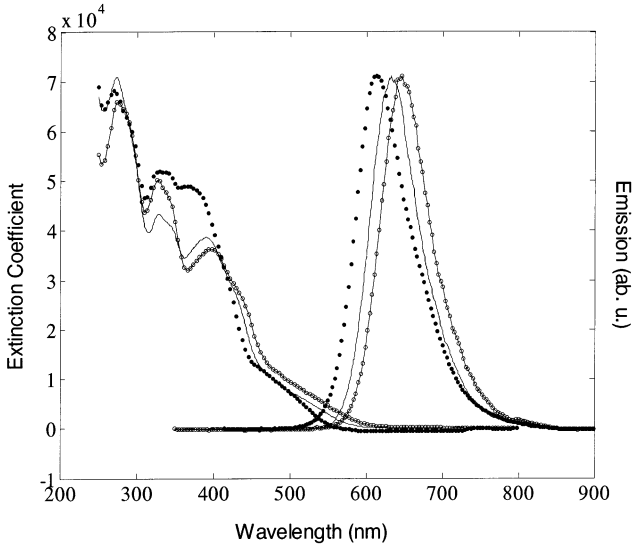


***Figure 12.*** Absorption ($\epsilon$) and emission of complexes **9** (○), **10** (●), and **11** (—).

ligand $\pi-\pi^*$ transition bands exhibit the strongest $\epsilon$ that is >60 000 L·cm$^{-1}$·mol$^{-1}$. Absorption bands that occur at roughly 390 and 500 nm are the $^1$MLCT and spin-forbidden $^3$MLCT bands. These are weaker bands with $\epsilon$ of 16 000 and 3700 L·cm$^{-1}$·mol$^{-1}$ for complex **1**. Extending the conjugation length of the polypyridyl ligand increases the strength of all absorption bands. Complexes **1**, **2**, and **3** are based upon ligand **21**. These have $\epsilon$ of 17 000 L·cm$^{-1}$·mol$^{-1}$ for the $^1$MLCT, 5000 L·cm$^{-1}$·mol$^{-1}$ for $^3$MLCT, and 70 000 L·cm$^{-1}$·mol$^{-1}$ for the LC state. Additional substitution or extending the conjugation length as in complexes **4**, **5**, and **6** affords $\epsilon$ of 28 000 L·cm$^{-1}$·mol$^{-1}$ for the $^1$MLCT, 11 000 L·cm$^{-1}$·mol$^{-1}$ for the $^3$MLCT, and 91 000 L·cm$^{-1}$·mol$^{-1}$ for the LC state. The same trends were observed for the phenanthroline-containing complexes (**7**, **8** vs **13**, **14**). With the extended conjugation in these systems, additional LC bands were observed between the main polypyridyl LC peak and the $^1$MLCT transition.

At room temperature the complexes feature smooth, unstructured exponential Gaussian emission typical of MLCT emission. The emission of the arsine complexes is to the red of the emission of the phosphine complexes. This offers the ability to tune the emission of Os(II) complexes by the use of different ligands to the specific application. Emission lifetime for the

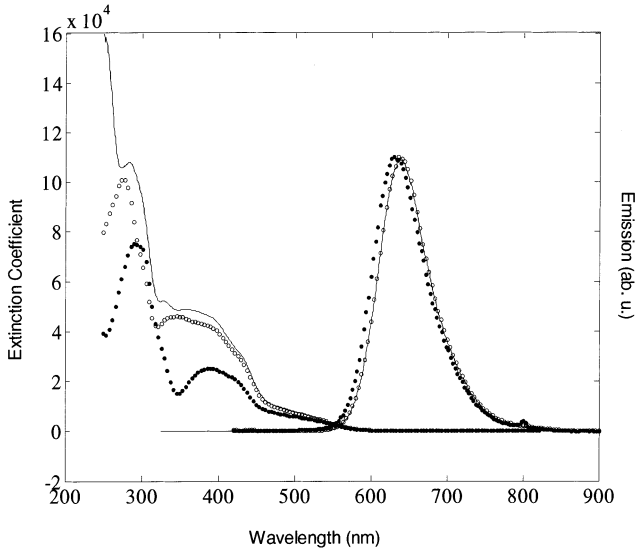


***Figure 13.*** Absorption ($\epsilon$) and emission of complexes **12** (●), **13** (○), and **14** (—).

bipyridyl complexes (**1**−**6**) were observed at roughly 450 ns, while the lifetimes for the phenanthroline complexes (**7**−**14**) were 1.2−2.0 $\mu$s. The difference in lifetime between the bipyridine- and phenanthroline-containing complexes may be due to the extended ring system of the phenanthroline. The complexes with arsine ligands (**23**, **25**) had shorter emission lifetimes than those with phosphine ligands (**24**). This may be due to the fact that arsenic is a heavier atom than phosphorus, thus increasing the rate of intersystem crossing and rate of phosphorescence. There was some effect of extending the conjugation length on the outer portion of the polypyridyl ligands and emission lifetime, as complexes with extended $\pi$ systems (**5**, **6**, **13**, and **14**) had slightly shorter emission lifetimes. The large spin−orbit coupling constant of osmium (~3500 $cm^{-1}$), and strong back-bonding between ligand and metal is resulting is short emission lifetime of the complexes with minor contributions from the arsenic, phosphorus, and the extended $\pi$ system. Complex **11** was the most efficient photoluminescence emitter with 45% quantum yield ($\Phi$), which is given by the following expression:

$$\Phi = \frac{k_p}{k_p + k_{nr} + k_q[Q]} \qquad (2)$$

where $k_p$ is the rate of radiative decay, $k_{nr}$ is the nonradiative decay rate, and $k_q$ is the quenching rate. A common quencher of luminescence is oxygen.

The 1,10-phenanthroline complexes had quantum yields in excess of 30%. The complexes with ligand **25** in general have greater quantum yields than the complexes with ligand **24**. This may be due to the heavy atom effect. From the lifetime data, complexes with arsine ligands have shorter lifetimes than complexes with phosphine ligands. The heavier arsenic increases spin−orbit coupling, which increases the rate of intersystem crossing. This may have the effect of making $k_p$ more competitive with $k_{nr}$ (eq 2) in the arsine complexes, thus increasing quantum yields of the complexes with ligand **25**. Osmium(II) complexes have been reported with quantum yields up to 24% in the literature.[14] The reported complexes are based upon ligand **24** and other non-phenyl-substituted bipyridyl ligands. The

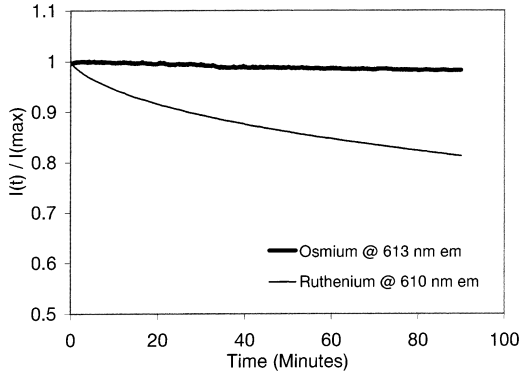


***Figure 14.*** Photodegradation of Ru(**22**)$_3$ and **7** in FIB7 polymer. Samples were illuminated for 90 min at 925 $\mu$W $cm^{-2}$.

complexes have a reported emission at 600 nm. Here we are reporting significantly red-shifted complexes (630−640 nm) with significantly greater quantum yields in seeming defiance of the energy gap law. The use of phenyl derivatives of 2,2′-bipyridyls and 1,10-phenanthrolines has been shown to increase quantum yields.[17] The radiative and nonradiative rate terms in the quantum efficiencies of Ru(II) complexes has also been discussed before.[17] An explanation of this phenomenon may be the reduction of bond vibrations and rotations that quench luminescence. C−H, N−H, and O−H bond vibrations and C−C bond rotations are well-known to quench luminescence. The increase in quantum yield by reduction in C−H bond vibrations is observable in this research report where complexes based upon ligand **23** (complexes **1**, **5**, and **9**) have significantly weaker quantum yield than similar complexes based upon ligand **25** (complexes **3**, **6**, and **11**). In the crystal structures given for complexes **3** and **12**, the phenyl groups are rotated out of the plane of the main polypyridyl structure. It has been shown[18] that phenyl groups on polypyridyl complexes become coplanar with the main polypyridyl structure in the excited state. This extends the $\pi$-system of the ligand, which hinders C−C bond rotation in the excited state. Thus, the use of phenyl groups reduces pathways (such as C−H bond vibration and C−C bond rotation) of nonradiative deactivation of the excited state.

**Photodegradation.** Illustrated in Figure 14 is a degradation comparison of Os complex **7** and Ru complex [Ru(**22**)$_3$$PF_6$]. After an exposure period of 90 min at 925 mW $cm^{-2}$ and 400 nm, the Os complex photo degraded 1%, while the Ru complex photodegraded 20% over the same time frame. This result can be explained by the energy levels of the metal-centered state for Ru(II) and Os(II) d6 octahedral complexes[36,49] as illustrated in Figure 15. Going down the periodic table affords an increase in the energy of the MC state of tris(polypyridyl) complexes of $Fe^{2+}$ to $Os^{2+}$. This is due to an increase in 10*Dq* value. For $Fe^{2+}$, the MC state is lowest in energy; thus, the polypyridyl complexes of $Fe^{2+}$ are nonluminescent and are easily formed and degrade. $Ru^{2+}$ has the MLCT state as the lowest in energy and the MC state is intermediate in energy between the LC and MLCT states; thus $Ru^{2+}$ complexes are luminescent. However, the low-lying MC state may be thermally populated, making it more susceptible to degradation and leading to loss in quantum yield with increasing temperature. Like $Ru^{2+}$, $Os^{2+}$ has the MLCT state as the lowest energy excited state. As $Os^{2+}$ is more easily oxidized than $Ru^{2+}$, the MLCT state is generally lower

(49) Demas, J. N.; DeGraff, B. A. *Anal. Chem.* **1991**, *63* (17), 829.

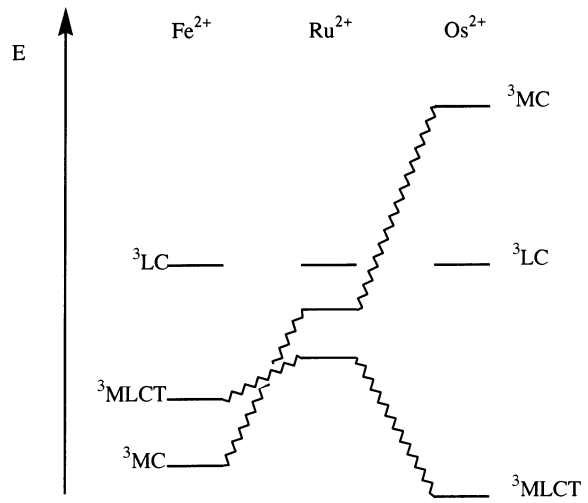


***Figure 15.*** Lowest triplet state orderings for group VIII divalent cations in octahedral symmetry. LC or MLCT as the lowest excited state leads to a luminescent compound; MC state as the lowest excited state leads to a nonluminescent compound.

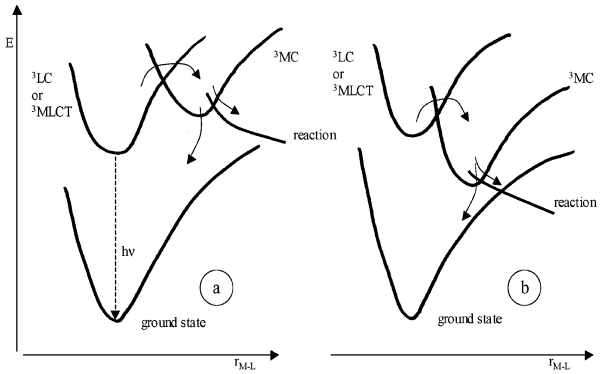


***Figure 16.*** Schematic representation of two limiting cases for the relative positions of the $^3$MC and $^3$LC (or $^3$MLCT) excited states.

in energy than the MLCT state for $Ru^{2+}$ compounds. The MC for $Os^{2+}$ compounds state is very high in energy, much higher than even the LC. Much more thermal energy is required to populate the MC state in polypyridyl $Os^{2+}$ compounds. Therefore the state is more difficult to populate, slowing the rate of photodegradation. Samples of Os(II) complexes **1**, **2**, **3**, **7**, and **8** in solution have been kept exposed to sunlight for over a year without change, while their Ru(II) counterparts degrade in just a few days.

Figure 16[50] illustrates the consequence of the positioning of the various excited states of the Os(II) or Ru(II) complexes. If the MLCT or LC state is lowest in energy, the resulting compound may be luminescent. However, if the MC state is lowest in energy, the resulting compound is not luminescent. Figure 16 illustrates that for the MLCT or LC states there is very little distortion along the metal−ligand bond axis, while for the MC state there is severe lengthening of the metal−ligand bonds. This is the result of the antibonding nature of the MC state. Once the MC state is populated, the complex may relax back to the ground state by nonradiative means, or the complex may lose a ligand and photoproducts result. The MC state is lower in energy for Ru(II) than for Os(II); hence, it is more easily populated. As a result, Ru(II) compounds degrade at a faster rate than their Os(II) counterparts. Another consequence of this is that $Ru^{2+}$ compounds exhibit greater loss in emission quantum yield with increasing temperature as shown in Table 6, where complexes **1**, **2**, **3**, **7**, and **8** are compared to two Ru(II) complexes, one that emits at 610 nm and one that emits at 673 nm. As temperature is increased, the MC state becomes more thermally populated, which leads to loss in quantum yield since the MC state relaxes by nonradiative means. As the MLCT is separated energetically from the MC state by red-shifting emission (or by increasing the energy of the MC state), the MC state becomes less populated, which leads to lower emission temperature dependence as observed in Table 6. The MC state of the Os(II) complexes is so high that the most blue-shifted (613 nm) Os(II) emitter (in Table 6) is less temperature-dependent than the most red-shifted (673 nm) Ru(II) emitter.

***Table 6.*** Temperature Dependence[a] of Osmium Complexes vs Ruthenium Complexes at 5−50 °C

| complex | X− | %/°C (760 Torr) | %/°C (vac) |
|---|---|---|---|
| **1** | HFB | −0.09 | −0.08 |
| **2** | Tf | −0.31 | −0.28 |
| **3** | Tf | −0.10 | −0.08 |
| **7** | Ts | −0.33 | −0.28 |
| **8** | Ts | −0.23 | −0.20 |
| Ru(**22**)$_3$ | $PF_6$ | −1.2 | −0.95 |
| Ru(**22**)$_2$DCBuBPY[b] | $PF_6$ | −0.48 | −0.44 |

[a] Loss of quantum yield with increasing temperature. [b] [Ruthenium-bis(**22**)-4,4′-bis(carboxybutyl ester)-2,2′-bipyridine]$^{2+}$. This compound has emission at 673 nm. We thank John Bullock (Central Washington State University) and Tim Hance for their generous supply of this compound.

**Organic LEDs.** The Os complexes demonstrate good phosphorescence efficiency and short excited-state lifetime (see Table 5), which are very desirable properties for light-emitting diode applications. To study the device performances of these complexes, double-layer devices were fabricated by doping the Os complexes at a weight ratio of 3 wt % into PVK:PBD or PVN:PBD blends. BTPD-PFCB was used as the hole-transporting layer. At the doping level of 3 wt %, the EL spectra of the devices are almost identical to the PL spectra of the Os complexes. No emission from the host materials was observed. Table 7 summarizes the performance of the devices. As can be seen, even with a simple double-layer structure and PVK:PBD as the host (type I devices), relatively good performances can be achieved. Among type I devices, the best external quantum efficiency of 0.78% was obtained from complex **11** with Ts as the counterion, while the highest brightness of 1430 cd/m$^2$ was obtained from complex **10** with Ts as the counterion. In general, the complexes utilizing arsine ligand **25** have better quantum yields than those with ligand **24**. Interestingly, the device efficiency follows this trend. It has been found that the Os complexes trap both electrons and holes, which facilitates the direct recombination of holes and electrons on the complex sites and benefits the device efficiency.[13] It should be noted that the counterion used in the complexes also affects the device performance, presumably through affecting the charge trap/transport property of the complex, thereby providing an additional way of tuning the device properties. Better external quantum effciencies were achieved from type II devices, where PVN:PBD was used as the host and excitation was transferred from the host more efficiently to the Os complex dopants,

(50) Juris, A.; Balzani, V.; Barigelletti, F.; Campagna, S.; Belser, P.; Zelewsky, A. *Coord. Chem. Rev.* **1988**, *84*, 85.

***Table 7.*** Performance of Os Complex Doped LEDs

| Os complex | $X^-$ | device[a] | $V_1$[b] (V) | $B_{max}$[c] (cd/m$^2$) | $\eta_{max}$[d] (%) |
|---|---|---|---|---|---|
| **1** | HFB | I | 9.3 | 310 | 0.64 |
| **2** | HFB | I | 7.5 | 260 | 0.27 |
| **2** | Ts | I | 8.7 | 970 | 0.27 |
| **3** | HFB | I | 7.6 | 410 | 0.60 |
| **3** | Ts | I | 7.5 | 725 | 0.42 |
| **4** | Tf | I | 8.4 | 600 | 0.32 |
| **6** | Tf | I | 6.7 | 799 | 0.28 |
| **7** | Tf | I | 6.9 | 750 | 0.20 |
| **8** | Tf | I | 6.4 | 1030 | 0.31 |
| **9** | Ts | I | 9.4 | 460 | 0.39 |
| **10** | Ts | I | 7.6 | 1430 | 0.48 |
| **11** | Ts | I | 8.0 | 1210 | 0.78 |
| **12** | Ts | I | 7.5 | 760 | 0.29 |
| **12** | $PF_6$ | I | 6.0 | 710 | 0.19 |
| **12** | $PF_6$ | II | 12.2 | 470 | 0.79 |
| **13** | Ts | I | 8.2 | 780 | 0.31 |
| **14** | Ts | I | 7.8 | 960 | 0.45 |
| **14** | $PF_6$ | I | 7.0 | 1090 | 0.48 |
| **14** | $PF_6$ | II | 14.2 | 870 | 2.2 |

[a] ITO/BTPD-PFCB/Os complex, PVK:PBD (∼45 nm)/Ca (type I), or ITO/BTPD-PFCB/Os complex, PVN:PBD(∼45 nm)/Ca (type II). [b] Voltage needed for brightness of 1 cd/m$^2$. [c] Maximum brightness. [d] Maximum external quantum efficiency.

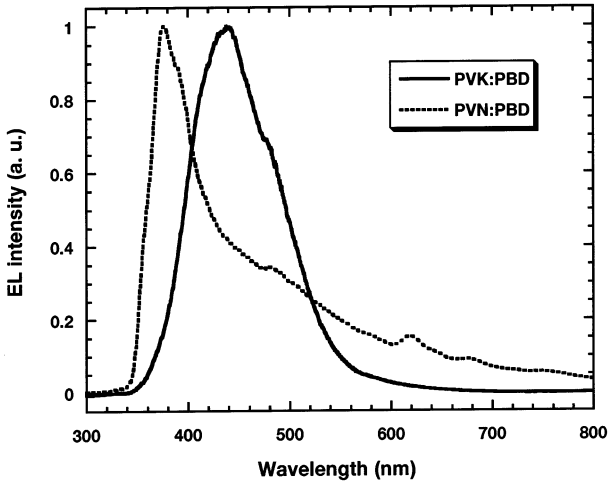


***Figure 17.*** Electroluminescent spectra of ITO/PVK:PBD/Ca and ITO/PVN:PBD/Ca devices.

presumably through a Förster mechanism. Figure 17 shows the EL spectra of ITO/PVK:PBD/Ca and ITO/PVN:PBD/Ca devices. As can be seen, compared with the EL emission of PVK:PBD host, the EL emission of PVN:PBD host peaks at shorter wavelength and provides a much better spectral overlap with the absorption spectra of the Os complexes. In Förster energy transfer, the energy transfer rate is proportional to the integral of the spectral overlap between the emission of the energy donor and the absorption of the energy acceptor. Therefore, PVN:PBD can transfer energy more efficiently to the Os complexes. Consequently, devices with a PVN:PBD host are more efficient than devices with a PVK:PBD host. It is very interesting to further compare the performance of complexes **12** and **14** doped type II devices. The maximum efficiency of a complex **14** doped PVN:PBD device is 2.2%, corresponding to a photometric efficiency of 1.9 cd/A, while that of a complex **12** doped PVN:PBD device is 0.79%. Substitution of Br in complex **12** with a naphthyl group in complex **14** almost doubles the extinction coefficient of $^1$MLCT absorption of the Os complex (see Table 5). A larger extinction coefficient contributes to a larger spectral overlap integral between the emission spectrum of PVN:PBD host and the absorption of complex **14**. This also contributes to a more efficient energy transfer from PVN:PBD to complex **14**. However, we note that compared to the devices based on PVN:PBD, the devices based on PVK:PBD have a lower turn-on voltage and higher brightness, mainly due to the better hole transport property of PVK. Nevertheless, the device data clearly demonstrate that Os complexes, when carefully designed, can be good candidates for light-emitting device applications.

OLEDs have been reported for ruthenium complexes with similar emission profiles as the Os(II) complexes being reported here. Various polymer host devices with emissions between 611 and 665 nm gave brightness in the range of 200−650 cd/m$^2$ and efficiency in the range of 0.08−2.5%.[51−53] In comparison, we report Os(II) devices that give efficiency up to 2.2% with a brightness of 870 cd/m$^2$ at 637 nm emission, or brightness of 1210 cd/m$^2$ with efficiency of 0.78% at 629 nm emission. The reported ruthenium complexes have emission quantum yields of 3.6−6.2%, significantly less than the reported osmium complexes here. At 611 nm emission we report a device with brightness of over 1400 cd/m$^2$ and efficiency of 0.48%.

## Conclusion

Red-emitting Os(II) complexes were synthesized for light-emitting applications from different ligand systems and counterions. These compounds feature strong MLCT absorption bands in the visible region and strong red phosphorescent emission ranging from 611 to 651 nm, with quantum yields up to 45%. The electronic structure and emission properties of the Os(II) complexes can be modified by changing the ligand structures. Electrophosphorescent devices were demonstrated by use of the Os complexes with doped PVK:PBD or PVN:PBD as the emitting layer. When PVK:PBD was used as the host matrix, brightness of over 1400 cd/m$^2$ was achieved. The best external quantum efficiency of 2.2%, which corresponds to a photometric efficiency of 1.9 cd/A, was achieved when PVN:PBD was used as the host matrix. It was found that the counterion also affects the performance of the complexes and devices, providing an additional way of tuning the material and device properties.

**Acknowledgment.** We thank the Air Force Office of Scientific Research (AFOSR) for support through the MURI and the DURIP program. A.K.-Y.J. thanks the Boeing-Johnson Foundation for financial support. B.C. thanks Professor Martin Gouterman for his help and guidance for several years. We thank Martin Sadilek and Ross Lawrence for their help with mass spectrometry.

**Supporting Information Available:** Synthesis and characterization data (PDF); X-ray crystallographic data (CIF). This material is available free of charge via the Internet at http://pubs.acs.org.

JA0176705

(51) Chan, W. K.; Ng, P. K.; Gong, X.; Hou, S. *Appl. Phys. Lett.* **1999**, *75*, 3920.
(52) Lee, J.; Yoo, D.; Rubner, M. F. *Chem. Mater.* **1997**, *9*, 1710.
(53) Rudmann, H.; Rubner, M. F. *J. Appl. Phys.* **2001**, *90* (9), 4338.